



OPEN Metabolomic insights of cultured meat compared to conventional meat

Heejung Park¹, IHyeon Cho¹, Sojeong Heo², Kisoo Han³, Young-jin Baek³, Wan-sup Sim³ & Do-Won Jeong²✉

The growing global demand for sustainable food sources has accelerated the development of cultured meat as an alternative to traditional animal-based meat. Cultured meat is produced through advanced cell cultivation techniques, offering potential solutions to environmental, ethical, and food security challenges. This study aims to predict the safety of cultured meat compared to conventional chicken using a comprehensive metabolomics approach. We conducted a comparative analysis of conventional chicken meat, muscle satellite cells, and myotube formed cells. The findings reveal that while the overall metabolic profiles of cultured and conventional meats are largely comparable, significant differences exist in specific metabolites associated with nutrient metabolism. These variations suggest potential differences in the nutritional content of cultured meat, which could affect its dietary value. Despite these differences, our analysis indicates no significant impact on the safety of cultured meat, which remains within acceptable safety limits. This study contributes to the ongoing evaluation of cultured meat as a viable and safe alternative in the pursuit of sustainable food sources.

Keywords Cultured meat, Metabolomics, Safety assessment, Metabolic pathway analysis, Network analysis

The global food industry faces significant challenges in addressing the rising demand for meat while simultaneously ensuring environmental sustainability and addressing animal welfare concerns¹. Additionally, there exists a growing disparity between the future demand for protein sources and the current capacity to supply meat². To bridge this gap, alternative meat products—developed through cellular agriculture and plant-based technologies—have emerged as promising solutions³. However, concerns regarding the safety and nutritional profile of alternative meat compared to conventional meat remain under scrutiny. A key barrier to the commercialization of cultured meat is the lack of systematic and comprehensive risk assessments^{4,5}. Metabolomics, a powerful tool for the comprehensive analysis of metabolites in biological systems, offers valuable insights for evaluating the biochemical implications of consuming cultured meat in comparison to traditional meat.

Metabolomics profiling has become a valuable tool for identifying key metabolic biomarkers following exposure to substances or pollutants, owing to its broad coverage, high sensitivity, and reproducibility⁶. This approach can detect subtle variations in the range of biological metabolites under different physiological or pathological conditions⁷. Additionally, metabolomics can uncover organismal responses to various internal and external environmental changes, as well as distinguishing phenotypic differences among individuals of the same species. Pathway enrichment analysis and metabolite-disease network analysis reveal functional impairments and highlight the connections between metabolites and related diseases⁸. These analyses help to elucidate the underlying biochemical pathways affected and the potential health implications associated with specific metabolic changes. Metabolomics has also shown significant promise in the field of safety assessment, especially in toxicology and medicine development⁹. Studies have demonstrated its capability to elucidate mechanisms of toxicity, identify early biomarkers, and improve preclinical safety evaluations. It provides a comprehensive overview of biochemical activity and cellular responses, helping to unravel adverse outcome pathways and improve the extrapolation of preclinical findings to humans. For example, the hepatotoxicity of triptolide, a compound from *Tripterygium wilfordii*, was investigated using LC-MS-based metabolomics, revealing significant changes in metabolites and identifying pathways related to liver injury medicine¹⁰. Similarly, the toxicity of *Dioscorea bulbifera* Rhizome was studied, identifying metabolites associated with liver toxicity and providing insights into the underlying mechanism.

¹Department of Foodservice Management and Nutrition, Sangmyung University, Seoul 03016, Republic of Korea.

²Department of Food and Nutrition, Dongduk Women's University, 60, Hwarang-ro 13-gil, Seongbuk-gu, Seoul 02748, Republic of Korea. ³Neo Cremar Co., Ltd, Seoul 06012, Republic of Korea. ✉email: jeongdw@dongduk.ac.kr

In the context of a growing global commercial market and increasing safety concerns for consumers, this study aims to conduct a safety and nutritional assessment of lab-cultured meat using a metabolomics-based approach. Technological method allows for the detection of subtle biochemical changes and potential toxicological markers that might not be evident through traditional safety assessment methods^{9–11}. We conducted a comparative metabolomic analysis of conventional chicken meat, muscle satellite cells, and myotube formed cells because there is currently a lack of research in this area. This study aims to fill the gap in knowledge by providing insights into the metabolic differences and similarities among these different cell types and conventional meat. By demonstrating a thorough understanding of the metabolic profile and ensuring the absence of harmful substances, producers can build trust and ensure the long-term safety of cultured meat products.

Method

To systematically analyze the metabolic profile of cultured meat in comparison to conventional chicken, we employed an untargeted metabolomics workflow. The overall experimental pipeline is summarized in Fig. 1.

Sample collection

For the comparative experiment, conventional meat, muscle satellite cells, and myotube formed cell. Conventional meats were purchased immediately after slaughter with the brisket of chickens raised in traditional farming (Harim, Iksan, Korea). To isolate chicken muscle satellite cells, leg muscles from 16-day-old chicken embryos were used. Briefly, the muscles were finely minced and digested with 0.1% pronase (Roche, Mannheim, Germany) at 37 °C for 80 min. After digestion, the supernatant was removed by centrifugation, and DMEM (Cytiva, Marlborough, USA) media supplemented with 10% FBS (Fetal bovine serum, Cytiva) and 1% P.S (Penicillin and streptomycin, Thermo Fisher Scientific, Waltham, USA) was added, followed by pipetting. The supernatant was then filtered through a 100 µm strainer and centrifuged. After removing the supernatant, growth medium [Ham's F10 (Cytiva) + 20% FBS + 1% P.S + 5 ng/ml human FGF2 (fibroblast growth factor 2, Miltenyi, Auburn, USA)] was added to the remaining muscle satellite cells, which were then cultured at 37 °C. And then, to obtain myotube formed cells, DMEM media supplemented with 2% FBS and 1% P.S was added into muscle satellite cells and incubated at 37 °C.

Metabolomics sample preparation

The samples were suspended in lysis buffer (50 mM ammonium bicarbonate), followed by sonication for 12 min at 15 °C using Covaris S2 Focused-Ultrasonicator (Covaris, Woburn, MA, USA). The concentration of protein was quantified using the Pierce BCA Protein Assay Kit (Thermo Fisher Scientific, Waltham, MA, USA). Metabolites were extracted from each 100 µg of protein sample by incubation with 4 volumes of cold methanol solution at –20 °C for 2 h. After centrifugation at 14,000×g for 10 min, the supernatant was transferred to a new 1.5 mL tube and completely dried using a speed-vac centrifugal vacuum concentrator (Vision Scientific, Daejeon, Korea). Dried metabolite contents were reconstituted in 100 µL of 0.1% formic acid in water. Reconstituted samples were transferred to autosampler vials and then subjected to LC-MS/MS analysis.

LC-MS/MS analysis

LC-MS/MS analysis for metabolomics was performed using a Q-Exactive Orbitrap hybrid mass spectrometer (Thermo Fisher Scientific, Waltham, MA, USA) along with an Vanquish UHPLC system (Thermo Fisher Scientific, Waltham, MA, USA). A 5 µL sample solution was injected into an Eclipse Plus C18 RRHD column (50 × 2.1 mm; id. 1.8 µm; Agilent, CA, USA) at 40 °C. The flow rate of the mobile phase was 0.2 mL/min. Analytes were eluted from the column under a gradient (solvent A, 0.1% formic acid in water; solvent B, 0.1% formic acid in 80% acetonitrile). The elution gradient was as follows: 2.5% B for 2 min, 2–12% B over 2–11 min, 12–28% B over 11–15 min; 28–60% B over 15–22 min; 96% B over 22–26 min; returned to 2.5% B for 5 min. Solvent A was run every sample as a blank solution. Mass spectrometer parameters were as follows: Full-MS scans, 100 to 1,000 (Positive mode) and 50 to 500 (Negative mode) m/z of scan range, 70,000 of resolution, 1×10^6 of AGC target, and maximum IT of 100 ms; For MS2 scans, the following parameters were used: 17,500 of resolution, 1×10^5 of AGC target, maximum IT was 200 ms, ± 2 m/z of isolation width, and NCE for dd-MS2 of 30; sheath gas flow rate was 19 (Positive mode) and 5 (Negative mode); aux gas flow rate was 1; spray voltage was 3.80 kV (Positive mode) and –3.40 kV (Negative mode); capillary temp was 320 °C; S-lens RF level was 60.0.

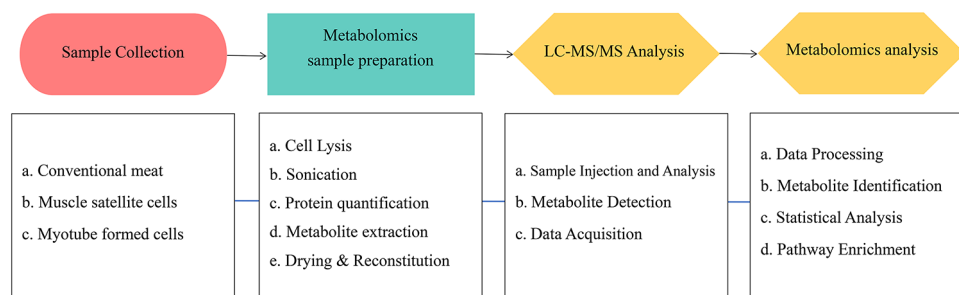


Fig. 1. Overview of the metabolomics workflow used in this study.

Metabolomics and chemometrics analysis

LC-MS/MS raw files were analyzed with Compound Discoverer 3.3™ (Thermo Fisher Scientific, Waltham, MA, USA). Analysis is performed in the 'Untargeted Metabolomics with Statistics Detect Unknowns with ID using online Data Base and mzlogic' mode. Compound identification is carried out using mzCloud (ddMS2, <https://www.mzcloud.org/>) and ChemSpider (formula or exact mass, <http://www.chemspider.com>), followed by ddMS2 data similarity searches for all compounds using mzCloud. According to the Metabolomics Standards Initiative (MSI) criteria, compounds are filtered at Level 2 (< 10 ppm, mzcloud score > 80) and Level 1 (ChemSpider < 5 ppm)¹². Metabolites with CV values of area exceeding 30% in QC (Pooled samples) are excluded, and duplicate metabolites are removed based on average area intensity. Based on the qualitative and quantitative analysis results of identified metabolites, statistical analysis is performed using MetaboAnalyst 6.0 (<http://www.metaboanalyst.ca>)¹³.

Results

Clustering and correlation analysis

In the positive mode, which is particularly suited for identifying compounds with basic functional groups, such as amines, and molecules that readily accept protons, the samples were basically clustered together according to the type of cultivation (Fig. 2A). The Venn diagram showed the number of common and unique metabolites in the two cultured groups (Fig. 2B). Compared to conventional meat, 45 common different metabolites existed in the two groups, which included diethanolamine, paracetamol, and acetylcholine, etc. Figure 2C displays clusters of different metabolites and their expression levels across each group. As well, this figure consists of 45 common different metabolites among the groups, and they exhibit similar expression trends. Figure 2D presents a correlation heat map utilized to screen for differential metabolites.

The negative ion mode, known for its effectiveness in analyzing acidic compounds such as carboxylic acids, phenols, and other molecules with acidic functional groups, did not reveal any clustering among the samples in this study (Fig. 3A). No significant differences in metabolites between the cultured groups. This suggests that the metabolite profiles of the test groups are similar with little to no variation. The Venn diagram showed the number of common and unique metabolites in the two cultured groups (Fig. 3B). Among them, 7 common different metabolites existed in the two groups, which included creatine, carnosine, and adenosine, etc. Figure 3C illustrated the clusters of different metabolites and their expression level. Additionally, this figure consists of 7 common different metabolites among the groups, and they show basically the same expression trends. Figure 3D is a correlation heat map used to screen for differential metabolites.

Metabolomics analysis

We established criteria to identify differential metabolites using thresholds of $p < 0.05$ and $VIP > 1$ (Table 1). In the positive ion mode, compared to conventional meat, the muscle satellite cells, and myotube-formed cells groups exhibited 66 and 69 different metabolites, respectively, with a fold change (FC) difference of 2 or more. In the negative ion mode, the muscle satellite cells, and myotube-formed cells groups showed 13 and 11 different metabolites, respectively, compared to conventional meat.

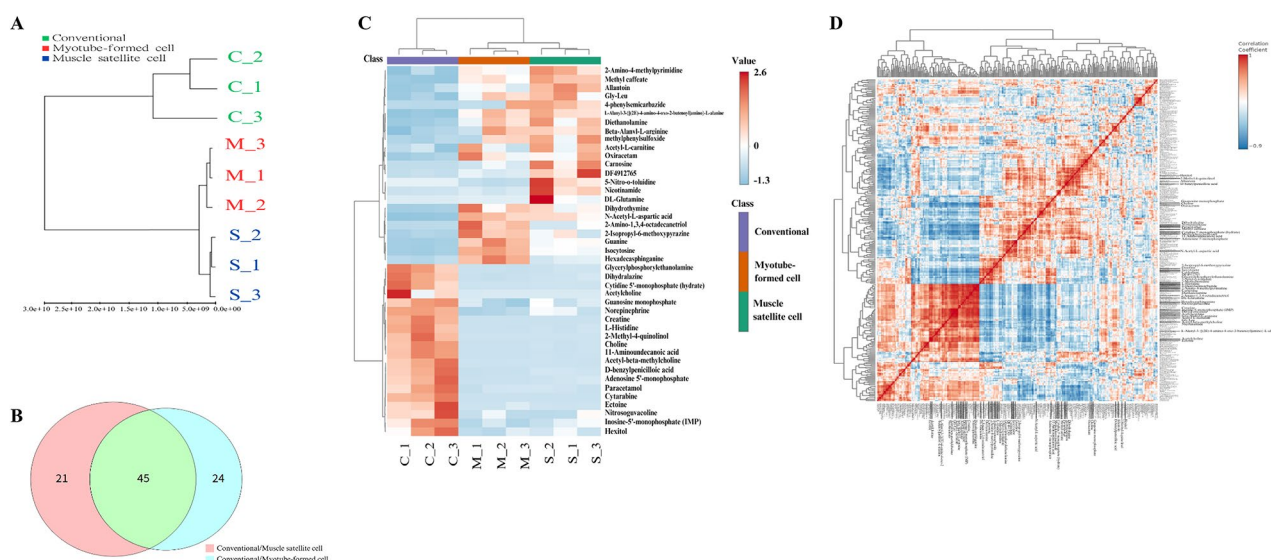


Fig. 2. Clustering and correlation analysis in positive mode. (A) The clustering dendrogram of cell type. (B) The number in different metabolites in cultured cell relative to the conventional meat (The filter conditions of differential metabolites are $p < 0.05$ and $VIP > 1$). (C) Heat map and clustering of the common different metabolites existed in the muscle satellite cells and myotube formed cell. (D) Correlation analysis and clustering heat map of all different metabolites, differential metabolites have been shown in bold.

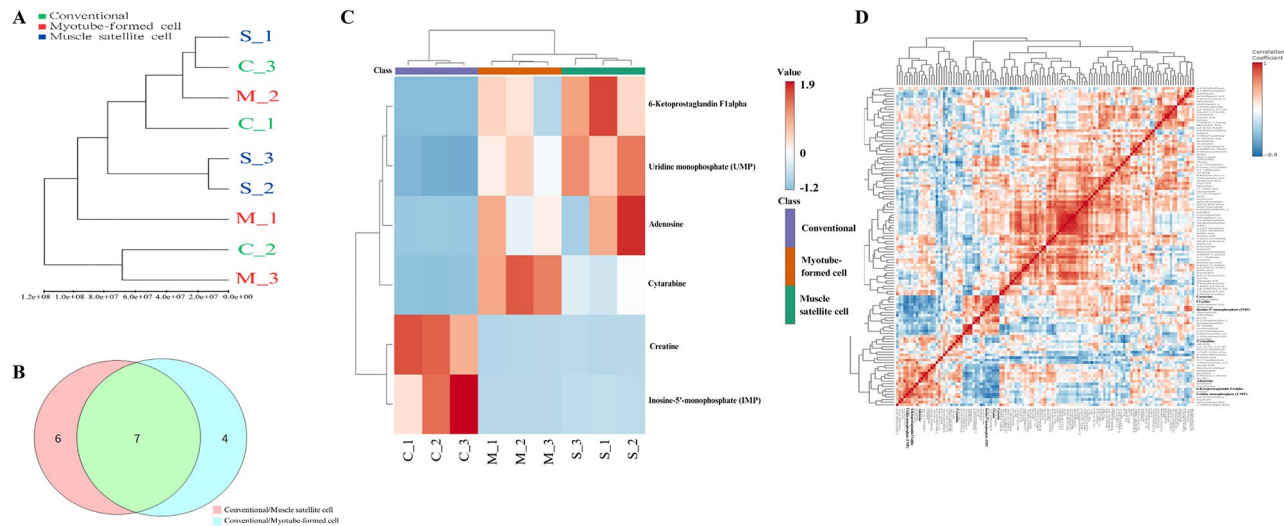


Fig. 3. Clustering and correlation analysis in negative mode. (A) The clustering dendrogram of cell type. (B) The number in different metabolites in cultured cell relative to the conventional meat (The filter conditions of differential metabolites are $p < 0.05$ and $VIP > 1$). (C) Heat map and clustering of the common different metabolites existed in the muscle satellite cells and myotube formed cell. (D) Correlation analysis and clustering heat map of all different metabolites, differential metabolites have been shown in bold.

Positive	Total	Up-regulation	Down-regulation
Positive mode			
MSC/con	66	32	34
MFC /con	69	34	35
Negative mode			
MSC /con	13	7	6
MFC /con	11	6	5

Table 1. Filtered differential metabolites by cultured type. * p -value < 0.05 , $FC > |2|$ * con : conventional. * MSC : muscle satellite cells. * MFC : myotube formed cells.

In muscle satellite cells, compared to conventional meat, several metabolites were found to be upregulated or downregulated. As a result, 32 upregulated and 34 downregulated metabolites were identified in the muscle satellite cell and visualized in a volcano plot (Fig. 4A). Representatively, metabolites including phosphoethanolamine, cytarabine, choline, and isocytosine were upregulated in the muscle satellite cell. Creatine and inosine-5'-monophosphate hypoxanthine were downregulated in the muscle satellite cell.

During the analysis in negative mode, 7 upregulated and 6 downregulated metabolites were identified in the muscle satellite cells and visualized in a volcano plot (Fig. 4B). Cytarabine (an anticancer drug), Monobutyl phthalate (a potentially endocrine-disrupting chemical), and Methyldopa (an anti-hypertensive drug) were detected.

In myotube-formed cells, metabolites were analyzed for up/down-regulation compared to conventional meat. As a result, 34 upregulated and 35 downregulated metabolites were identified in the myotube-formed cells and visualized in a volcano plot (Fig. 5A). Metabolites include levofloxacin, cytarabine, MTIC (5-(3-Methyl-1-triazeno) imidazole-4-carboxamide), diethanolamine, and furfural. Some metabolites are reported to cause tingling and corrosion due to acidity but are also naturally present in the body or consumed in food. In negative mode analysis of metabolites, 6 upregulated and 5 downregulated metabolites were identified in the myotube-formed cells and visualized in a volcano plot (Fig. 5B). Metabolites related to nucleic acids were predominantly detected. Cytarabine, UMP, and creatine were also detected in myotube-formed cells, just as it was in muscle satellite cells.

We analyzed the metabolites present in muscle satellite cells and myotube-formed cells and compared them to those of conventional meat using the HMDB classification (Table 2). The total metabolites were composed of amino alcohols ($n=2$), amino acids and derivatives ($n=15$), fatty acids and derivatives ($n=10$), aromatic compounds and benzenoids ($n=9$), steroids and related compounds ($n=2$), nucleotide and related compound ($n=14$), phosphate and phosphoesters ($n=5$), carboxylic acid and derivatives ($n=6$), heterocyclic compounds ($n=8$), quaternary ammonium compounds ($n=2$), organosulfur compounds ($n=1$), antibiotics ($n=1$), peptide and related compound ($n=3$), alcohols ($n=2$), and miscellaneous compounds ($n=2$). Among them, amino acids, peptide, organic chemicals, fatty acid, steroids, and alcohols, which are known to have no impact on safety.

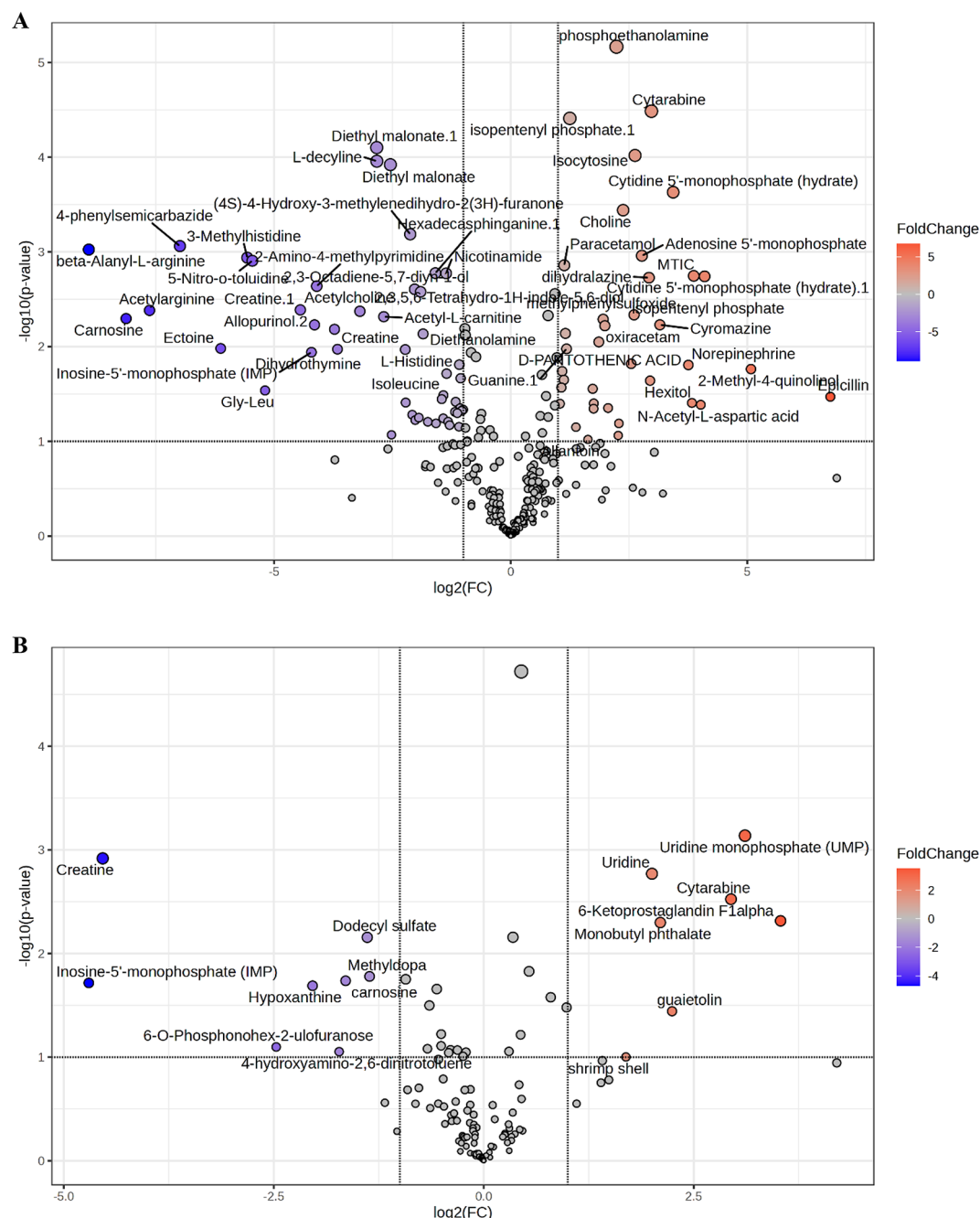


Fig. 4. Volcano plot of muscle satellite cells versus conventional meat. (A) positive mode (B) negative mode. Selected metabolites are annotated in the graphs. Dotted horizontal line indicates threshold for p value of 0.01 and the dotted vertical lines indicate thresholds for ± 2 -fold changes.

Aromatic compounds and benzenoids are environmental pollutants that can potentially trigger allergic reactions in certain individuals, depending on their sensitivity. However, these substances are also used as food additives, where they have been proven safe and are approved for use¹⁴. Additionally, there are nucleotide, phosphate, carboxylic acid, and ammonium compounds, which are known to be involved in maintaining physiology or nutrient^{15–17}.

Metabolic pathway enrichment

The enrichment analysis of metabolic pathways for muscle satellite cells of filtered differential metabolites was conducted using the Kyoto Encyclopedia of Genes and Genomes (KEGG) database¹⁸ (Fig. 6A and C) and the Small Molecule Pathway Database (SMPDB) (Fig. 6B and D).

Figure 6A shows the top 25 enriched metabolic pathways identified using the KEGG database¹⁸ under positive ion mode. Larger and darker red dots indicate pathways with higher statistical significance (smaller p -values). Key

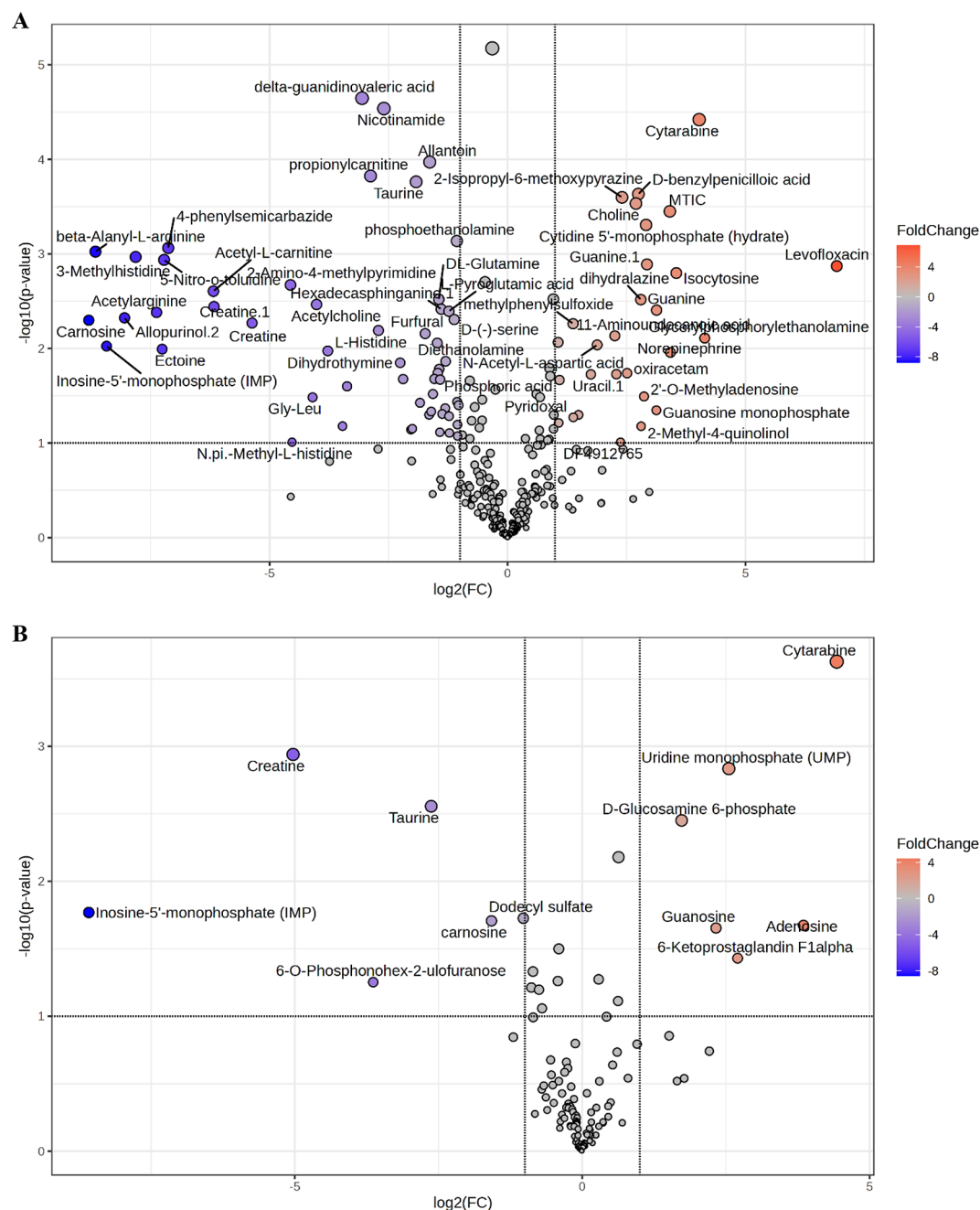


Fig. 5. Volcano plot of myotube formed cells vs. conventional meat. (A) positive mode (B) negative mode. Selected metabolites are annotated in the graphs. Dotted horizontal line indicates threshold for p value of 0.01 and the dotted vertical lines indicate thresholds for ± 2 -fold changes.

pathways identified include beta-alanine metabolism, histidine metabolism, and purine metabolism, reflecting significant differences between the groups. Highlights enriched pathways identified using the KEGG database under negative ion mode was shown in Fig. 6B. Pathways such as purine metabolism, histidine metabolism, and glycine, serine, and threonine metabolism are prominent. Metabolic pathways analyzed using the SMPDB database under positive ion mode was displayed in Fig. 5C. Enrichment analysis identifies significant pathways similar to those in Fig. 6A, including beta-alanine metabolism, histidine metabolism, and purine metabolism. Figure 6D focuses on pathways enriched in the SMPDB database under negative ion mode. Pathways such as purine metabolism, betaine metabolism, and selenometabolism are emphasized.

Metabolic pathway enrichment analysis for filtered differential metabolites between the conventional meat and myotube-formed cells are shown in Fig. 7. This figure presents the results of metabolic pathway enrichment analysis, visualized as dot charts, to identify significant metabolic pathways in positive and negative ion modes using the KEGG¹⁸ and SMPDB databases. Positive ion mode results using the KEGG database¹⁸. Pathways such as histidine metabolism, purine metabolism, and beta-alanine metabolism show significant enrichment, with

Classification	Muscle satellite cell		Myotube formed cell	
	Positive mode	Negative mode	Positive mode	Negative mode
Amino Alcohols	Diethanolamine 2-Amino-1,3,4-octadecanetriol		Diethanolamine	
Amino Acids and Derivatives	Oxiracetam Creatine N-Acetyl-L-aspartic acid L-Histidine 3-Methylhistidine Isoleucine DL-Glutamine Nicotinamide Ectoine Acetylarginine	Creatine Dodecyl sulfate	Oxiracetam Creatine N-Acetyl-L-aspartic acid L-Histidine N,pi-Methyl-L-histidine 3-Methylhistidine DL-Glutamine L-Lysine Ectoine Benzylpenicilloic acid Acetylarginine Stachydrine	Creatine
Fatty Acids and Derivatives	L-Carnitine Ester Acetyl-L-carnitine Acetylcholine 2,3-Octadiene-5,7-diy-1-ol 2-Isopropyl-6-methoxypyrazine		Propionylcarnitin Acetyl-L-carnitine Acetylcholine 3-oxopalmic acid 10,16-Dihydroxyhexadecanoic acid 8-Amino-7-oxononanoic acid Delta-guanidinovaleic acid	
Aromatic Compounds and Benzenoids	Paracetamol Methylphenylsulfoxide DF4912765 Norepinephrine	Monobutyl phthalate Methyldopa	Paracetamol Piperonylic Acid Phenylglyoxylic acid Norepinephrine 2-Isopropyl-6-methoxypyrazine Levofloxacin	
Steroids and Related Compounds	11-Aminoundecanoic acid	6-Ketoprostaglandin F1alpha	11-Aminoundecanoic acid	6-Ketoprostaglandin F1alpha
Nucleotides, Nucleosides, and Related Compounds	Guanosine monophosphate Adenosine 5'-monophosphate Inosine-5'-monophosphate (IMP) Guanine Cytarabine Cytidine 5'-monophosphate (hydrate)	Adenosine IMP Cytarabine Uridine UMP	Beta-Nicotinamide mononucleotide Nicotinamide 2'-O-Methyladenosine Inosine Guanosine monophosphate Adenosine 5'-monophosphate IMP Guanine Cytarabine Cytidine 5'-monophosphate (hydrate)	Adenosine, Guanosine Inosine-5'- monophosphate (IMP) Cytarabine Uridine monophosphate (UMP)
Phosphates and Phosphoesters	Isopentenyl phosphate Phosphoethanolamine Glycerolphosphorylethanolamine		Phosphoric acid Glycerolphosphorylethanolamine	D-Glucosamine 6-phosphate
Carboxylic Acids, Amides, and Derivatives	Diethyl malonate D-(+)-Tryptophan Succinimide Citric acid		MTIC 5-Ethyl-4-hydroxy-3(2 H)-furanone	
Heterocyclic Compounds	Allantoin Allopurinol Uracil Dihydrothymine Dihydralazine		Allantoin (+)-D-Isosorbide Pyridoxal Dihydrothymine zopiclone dihydralazine	
Quaternary Ammonium Compounds	Choline		Choline	
	Acetyl-beta-methylcholine		Acetyl-beta-methylcholine	
Organosulfur Compounds	-		Taurine	Taurine
Antibiotics	Epicillin			
Peptides and Related Compounds	Carnosine beta-Alanyl-L-arginine	Carnosine	beta-Alanyl-L-arginine Carnosine Gly-Leu	Carnosine
	Gly-Leu			
Alcohols	D-Pantothenic acid		Hexitol	
	Hexitol			
Miscellaneous Compounds	Cyromazine	Hypoxanthine		

Table 2. Metabolites clustered into chemical classes according to HmDB classification. L-Carnitine Ester: 3-[(2,6-Dimethylheptanoyl)oxy]-4-(trimethylammonio)butanoate. MTIC: 5-(3-Methyl-1-triazeno) imidazole-4-carboxamide.

larger dots representing higher enrichment ratios and smaller p-values indicating greater statistical significance (Fig. 7A). Notable pathways identified in the negative ion mode using the KEGG database¹⁸ include purine, hypotaurine, taurine glycine, serine, and threonine metabolism (Fig. 7B). Positive ion mode results using the SMPDB database (Fig. 7C). Enriched pathways include histidine metabolism, purine metabolism, and beta-

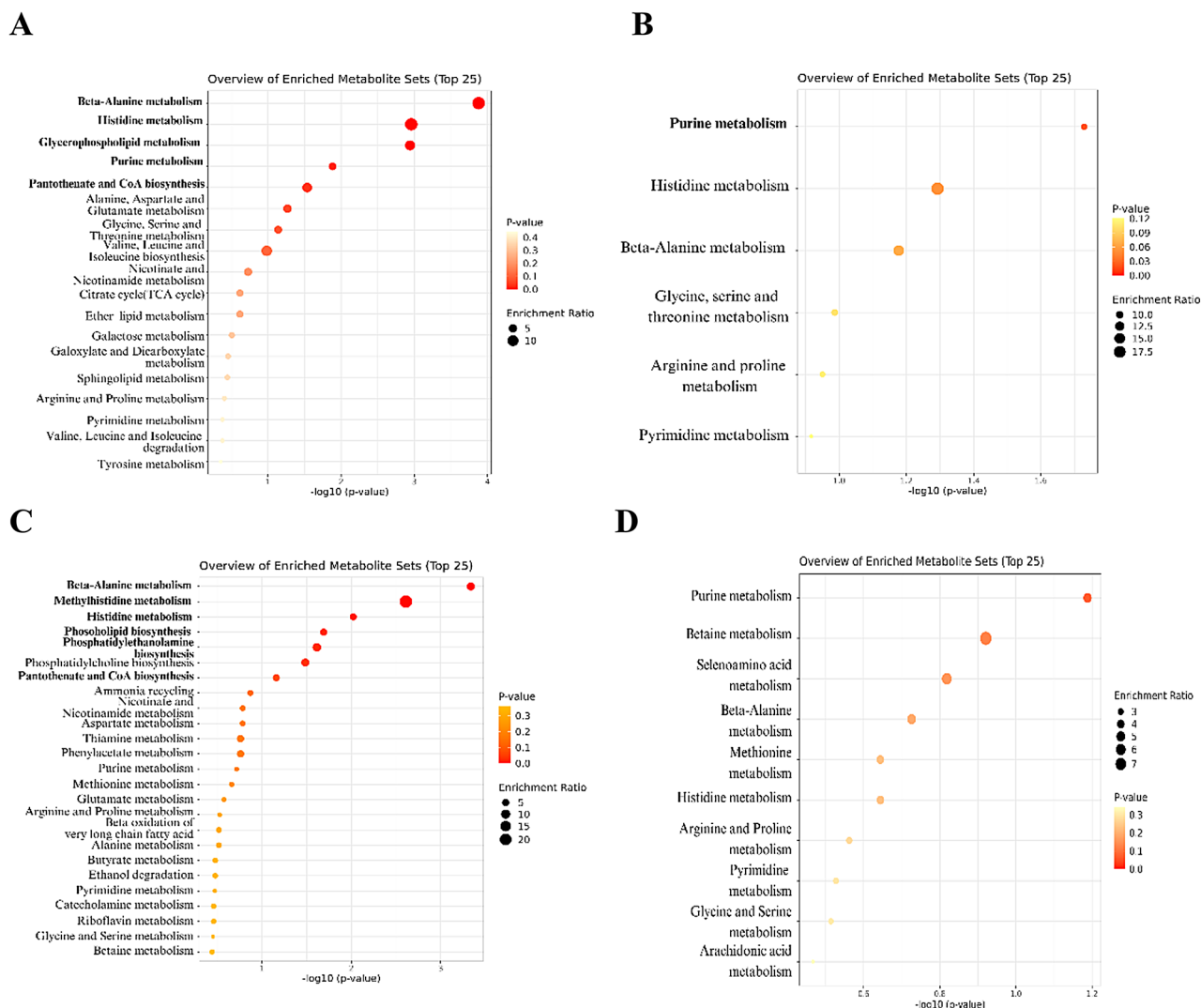


Fig. 6. Metabolic pathway enrichment analysis for filtered differential metabolites between conventional group and muscle satellite cell group. Dot chart in positive mode (A) and negative mode (B) by KEGG database; Dot chart in positive mode (C) and negative mode (D) by SMPDB database.

alanine metabolism, consistent with KEGG¹⁸ analysis. The results using the SMPDB database, taurine and hypotaurine metabolism, purine metabolism, and selenometabolism emerge as significantly enriched pathways in the negative ion mode (Fig. 7D).

According to KEGG¹⁸, significant enrichments were observed in pathways including sphingolipid metabolism, glycerophospholipid metabolism, nicotinate and nicotinamide metabolism, beta-alanine metabolism, and histidine metabolism. SMPDB highlighted pathways such as arginine and proline metabolism, glycine, serine and threonine metabolism, pyrimidine metabolism, pantothenate and CoA biosynthesis, purine metabolism, and beta-alanine metabolism (Table 3). For the myotube-formed cells, according to KEGG¹⁸, significant enrichments were observed in pathways including primary bile acid biosynthesis, beta-alanine metabolism, arginine and proline metabolism, glycine, serine and threonine metabolism. SMPDB highlighted pathways such as taurine and hypotaurine metabolism, bile acid biosynthesis, methionine metabolism.

Network analysis

For the muscle satellite cell, the inclusion of energy-related molecules like adenosine triphosphate (ATP), adenosine monophosphate (AMP), and creatine underscores the diagram's focus on energy metabolism, with phosphorylation processes being evident through the connections to ribose-1-phosphate and guanosine diphosphate (Fig. 8A and B). The diagram also shows interactions with cofactors like sodium and magnesium, which are crucial for stabilizing nucleotide structures and facilitating enzymatic reactions. The presence of specialized metabolites such as methyl dopa and 6-hydroxydopamine suggests links to neurotransmitter metabolism or specific drug metabolism pathways, further reflecting the complexity of the interconnected biochemical processes in the network. In the negative mode, the network illustrates the complex interplay

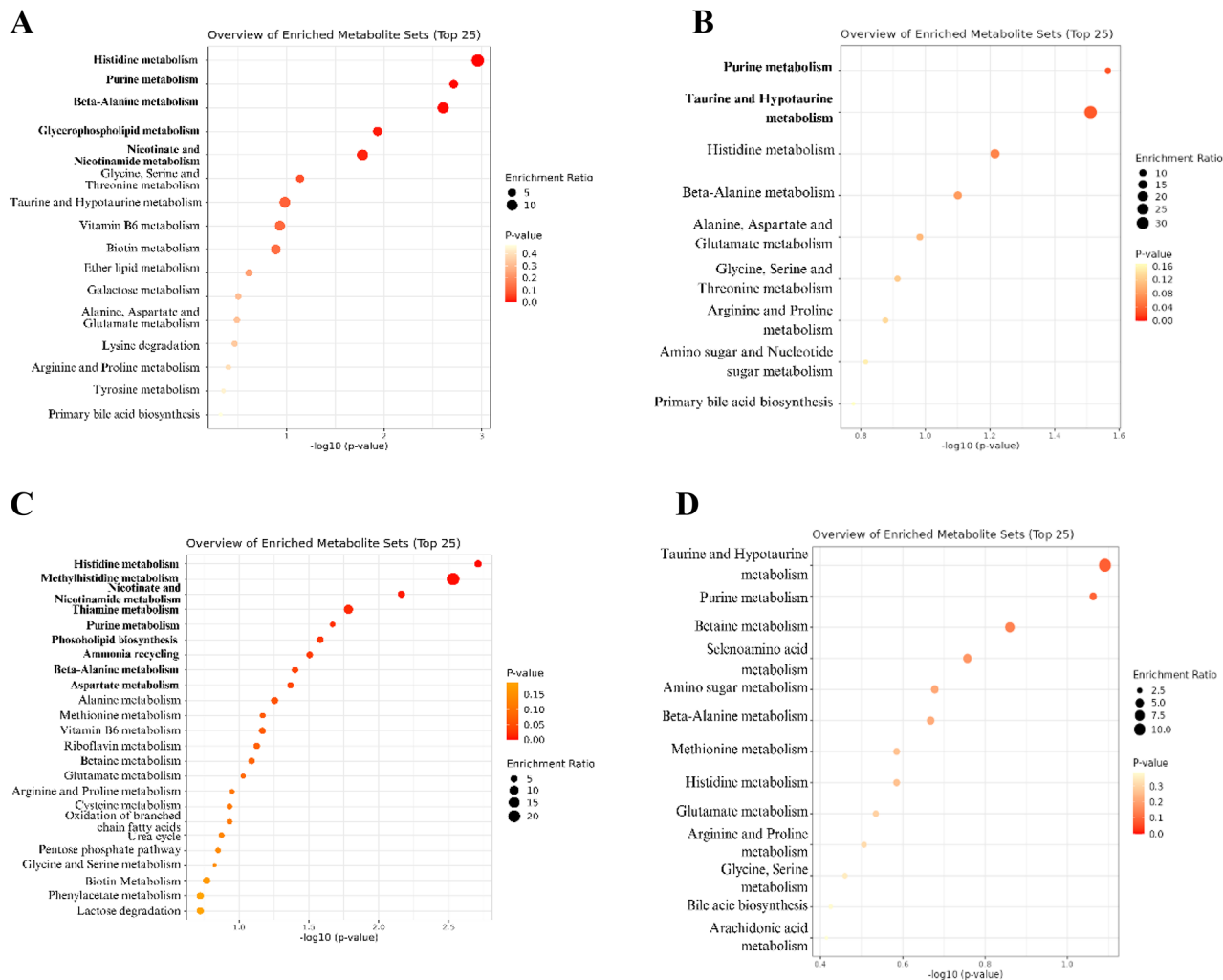


Fig. 7. Metabolic pathway enrichment analysis for filtered differential metabolites between conventional group and myotube formed cell group. Dot chart in positive mode (A) and negative mode (B) by KEGG database(Kanehisa et al., 2025); Dot chart in positive mode (C) and negative mode (D) by SMPDB database.

Muscle satellite cell		Myotube-formed cell	
KEGG database	SMPDB database	KEGG database	SMPDB database
Positive mode			
beta-Alanine metabolism	Methylhistidine metabolism	Histidine metabolism	Methylhistidine metabolism
Histidine metabolism	Phosphatidylethanolamine biosynthesis	beta-Alanine metabolism	Thiamine Metabolism
Glycerophospholipid metabolism	beta-Alanine metabolism	Nicotinate and nicotinamide metabolism	Histidine metabolism
Purine metabolism	Phospholipid biosynthesis	Glycerophospholipid metabolism	Nicotinate and Nicotinamide metabolism
Pantothenate and CoA biosynthesis	Histidine metabolism	Purine metabolism	Phospholipid biosynthesis
	Pantothenate and CoA biosynthesis		Ammonia recycling
			Beta-Alanine metabolism
			Aspartate metabolism
			Purine metabolism
Negative mode			
Purine metabolism	–	Purine metabolism	–
		Taurine and hypotaurine metabolism	–

Table 3. Enriched pathways by two different databases for MSC and MFC.

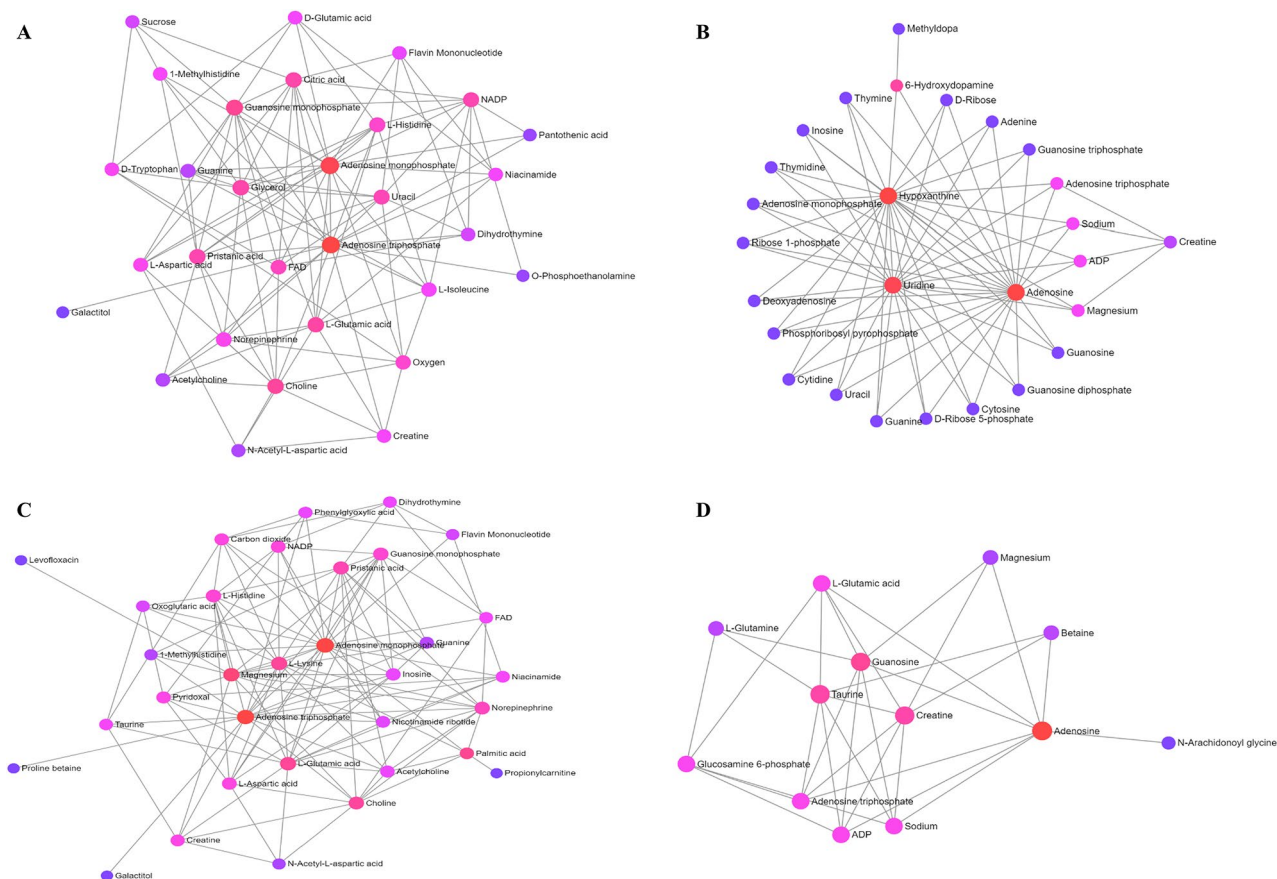


Fig. 8. Network analysis for connection between metabolites. MetaboAnalyst 6.0 was applied to generate connection maps. Connection map of muscle satellite cells in positive mode (A) and negative mode (B); connection map of myotube formed cells in positive mode (C) and negative mode (D).

between energy production, amino acid metabolism, and nucleotide synthesis, showcasing how these processes are tightly integrated to maintain cellular function (Fig. 8B).

Figure 8C and D shows a metabolic network diagram highlighting the interactions between various metabolites with a focus on energy metabolism, amino acid metabolism, and nucleotide metabolism in the myotube foamed cells. The larger, red nodes like ATP, AMP, and guanosine monophosphate (GMP) appear to be central metabolites. These molecules play crucial roles in energy transfer, signaling, and nucleotide synthesis in cellular metabolism (Fig. 8C). The connections around AMP and ATP suggest a focus on nucleotide metabolism, which is crucial for processes such as DNA and RNA synthesis, as well as energy metabolism. The presence of amino acids like L-aspartic acid, L-isoleucine, and others like creatine and choline, shows the network's inclusion of both structural components of proteins and molecules involved in cellular signaling and membrane structure. The lines connecting metabolites like citric acid, which is a key component of the citric acid cycle (Krebs cycle), to other compounds highlight the interconnected nature of metabolic pathways. This cycle is essential for energy production in the form of ATP. Metabolites such as NADP and FAD, which are coenzymes, are essential for redox reactions, indicating that this network might also highlight oxidative metabolism. Central metabolites such as ATP and AMP are prominent, reflecting their critical roles in cellular energy transfer and signaling processes. Magnesium and L-lysine are also central, playing essential roles in stabilizing ATP and participating in protein synthesis.

Discussion

Metabolomics, focusing on the comprehensive analysis of metabolites in biological systems, has become a critical tool in evaluating food safety^{19,20}. Recent developments for non-targeted food authenticity such as metabolomics have significantly advanced the capabilities of food metabolomics, enhancing its role in verifying the safety of food products²¹. These emerging trends and applications provide deeper insights into metabolic pathways and their implications for food safety²². By leveraging advanced analytical techniques such as Liquid Chromatography-Mass Spectrometry (LC-MS/MS), researchers can uncover detailed biochemical profiles in food products^{23,24}. For example, LC-MS/MS is known for its sensitivity and broad metabolite coverage, plays a pivotal role in profiling complex matrices like fermented cereals and irradiated meats, offering insights into food safety and quality^{25,26}. Additionally, spatial metabolomics using LC-MS has revealed significant metabolic differences in red and white muscles of rabbit meat, contributing to the understanding of muscle-specific

metabolic functions²⁷. This approach not only supports regulatory frameworks but also contributes to the development of safer, high-quality food products by providing reliable data for safety assessments^{11,28}. Similarly, the integration of mass spectrometry-based metabolomics in food science assures food traceability, thereby enhancing consumer protection^{6,29}. Consequently, metabolomics can elucidate microbial metabolic pathways, supporting food safety by identifying its metabolic consequences^{7,30}. This overall process in metabolomics offers significant benefits in ensuring food safety and quality^{9,10,31}, highlighting its broader applications in the evaluation of cultured meat safety.

The results of this study provide crucial insights into the metabolic profiles of muscle satellite cells and myotube formed cells, revealing how different cultivation conditions influence these profiles and the potential implications for cellular function and safety. The clustering and correlation analysis in positive ion mode demonstrates that the samples cluster well according to cultivation type, indicating distinct metabolic profiles for each group. This finding suggests that the cultivation environment significantly impacts the metabolic state of the cells. The identification of 45 common metabolites, such as diethanolamine, paracetamol, and acetylcholine, highlights key metabolic changes associated with cultivation. These metabolites are likely involved in critical cellular processes such as neurotransmission and cellular signaling, which may be influenced by the cell culture environment. The consistent expression trends observed across these metabolites further support the robustness of the metabolic shifts induced by cultivation conditions.

In contrast, the negative ion mode did not show significant clustering, indicating that the metabolite profiles across the test groups are relatively similar. This lack of differentiation suggests that the metabolic alterations observed in the positive mode may be more specific to certain pathways or conditions that are not as pronounced in the negative mode.

The metabolomics analysis reveals a dynamic metabolic landscape in both muscle satellite cells and myotube-formed cells, with numerous metabolites showing significant upregulation or downregulation. In muscle satellite cells, the upregulation of metabolites like phosphoethanolamine and cytarabine suggests heightened activity in pathways related to membrane synthesis and nucleotide metabolism, which are crucial for rapid cell division. The downregulation of creatine and inosine-5'-monophosphate, on the other hand, may reflect a shift away from energy storage and towards immediate energy consumption, a characteristic of proliferating cells. The identification of potentially hazardous metabolites, such as Levofloxacin and 5-Nitro-o-toluidine, in myotube-formed cells raises concerns about the safety of cultured cells under certain conditions. These findings underscore the importance of rigorous safety assessments, particularly when considering cultured cells for food production or therapeutic use. The detection of cytarabine and guanosine in the negative ion mode further highlights the need for careful monitoring of metabolites that could pose health risks.

The pathway enrichment analysis underscores the complexity of the metabolic changes associated with cell differentiation. The enrichment of pathways such as sphingolipid metabolism and glycerophospholipid metabolism indicates significant alterations in membrane composition and function, which are essential for maintaining cellular integrity during differentiation. The involvement of amino acid metabolism pathways, including glycine, serine, and threonine metabolism, suggests a shift towards biosynthetic activities necessary for protein synthesis and cellular growth. These findings highlight the intricate balance between energy production, biosynthesis, and cellular maintenance in differentiated cells. The observed enrichments in pathways like purine metabolism and pantothenate and CoA biosynthesis further emphasize the centrality of nucleotide and coenzyme metabolism in supporting the energetic and biosynthetic demands of differentiating cells.

The network analysis provides a comprehensive view of the interconnected metabolic processes in muscle satellite cells and myotube-formed cells. The centrality of metabolites like ATP, AMP, and GMP underscores their pivotal roles in energy metabolism, signaling, and nucleotide synthesis. These metabolites serve as hubs in the network, connecting various metabolic pathways and facilitating the coordination of cellular activities. The presence of amino acids like L-aspartic acid and L-isoleucine, alongside energy-related molecules like creatine and choline, reflects the network's focus on supporting both the structural and functional demands of cells. The identification of specialized metabolites such as methyl dopa and 6-hydroxydopamine suggests that differentiation may involve unique metabolic pathways related to neurotransmitter synthesis or drug metabolism, adding another layer of complexity to the cellular metabolic landscape.

One limitation of this study is the relatively small sample size, which may affect the generalizability of the findings. However, as this is the first study to investigate the fundamental metabolic changes in cultured meat, our primary aim was to explore the baseline metabolic alterations rather than to derive definitive conclusions requiring a larger sample size. Future studies with larger sample sizes are warranted to further confirm and expand upon our findings, providing a more comprehensive understanding of the metabolic changes involved in cultured meat production.

In addition, consumer acceptance of cultured meat may be influenced by both perceived safety and nutritional benefits. Any metabolic differences identified in our study could raise questions regarding equivalence to conventional meat, making it essential to clearly communicate metabolomic data in a transparent and accessible manner. However, it is important to recognize that metabolic differences do not necessarily indicate a safety risk, as variations in metabolite composition are expected due to differences in the cultivation process. As long as safety is thoroughly assessed and validated, these metabolic variations should not pose a concern for consumer health or regulatory approval.

To address these concerns, additional studies—including larger-scale clinical trials, long-term feeding studies, and expanded metabolomics analyses with diverse meat types—would be beneficial to further validate safety and nutritional equivalence. Continued research, along with engagement with regulatory bodies and clear public communication, will be key factors in ensuring successful adoption of this novel food product. Providing robust scientific evidence on the safety and quality of cultured meat is essential for both regulatory approval and public acceptance.

Conclusion

The metabolomic analysis revealed differences between cultured cells and conventional meat, suggesting variations in their metabolic profiles. However, these differences do not seem to pose toxicity concerns. Although antibiotics were detected in some cases, this is likely due to components in the cell culture medium rather than an inherent issue with the cultured cells themselves. The impact on amino acid, peptide, and fatty acid metabolism indicates that the nutrient content in the final cultured product might differ from that of conventional meat. These findings suggest that while cultured meat may offer a viable alternative, its nutritional composition could vary, necessitating further optimization to match or enhance the nutritional value of traditional meat products.

Data availability

Data is available at the NIH Common Fund's National Metabolomics Data Repository (NMDR) website, the Metabolomics Workbench, <https://www.metabolomicsworkbench.org>, where it has been assigned Project ID PR002228. The data can be accessed directly via its Project DOI: 10.21228/M8MZ51.

Received: 24 December 2024; Accepted: 30 April 2025

Published online: 05 May 2025

References

- Lynch, J. & Pierrehumbert, R. Climate impacts of cultured meat and beef cattle. *Front. Sustain. Food Syst.* **3**, 5; (2019). <https://doi.org/10.3389/fsufs.2019.00005>
- Smith, K. et al. Meeting the global protein supply requirements of a growing and ageing population. *Eur. J. Nutr.* **63**, 1425–1433. <https://doi.org/10.1007/s00394-024-03358-2> (2024).
- van Vliet, S. et al. A metabolomics comparison of plant-based meat and grass-fed meat indicates large nutritional differences despite comparable nutrition facts panels. *Sci. Rep.* **11**, 13828. <https://doi.org/10.1038/s41598-021-92309-5> (2021).
- Gu, Y., Li, X. & Chan, E. C. Y. Risk assessment of cultured meat. *Trends Food Sci. Technol.* **138**, 491–499. <https://doi.org/10.1016/j.tifs.2023.06.037> (2023).
- Fraeye, I., Kratka, M., Vandeburgh, H. & Thorrez, L. Sensorial and nutritional aspects of cultured meat in comparison to traditional meat: much to be inferred. *Front. Nutr.* **7**, 35. <https://doi.org/10.3389/fnut.2020.00035> (2020).
- Wang, H. et al. Recommendations for improving identification and quantification in non-targeted, GC-MS-based metabolomic profiling of human plasma. *Metabolites* **7**, 45. <https://doi.org/10.3390/metabo7030045> (2017).
- Pasikanti, K. K., Ho, P. C. & Chan, E. C. Gas chromatography/mass spectrometry in metabolic profiling of biological fluids. *J. Chromatogr. B* **871**, 202–211. <https://doi.org/10.1016/j.jchromb.2008.04.033> (2008).
- Lei, X. & Tie, J. Prediction of disease-related metabolites using bi-random walks. *PLoS One* **14**, e0225380. <https://doi.org/10.1371/journal.pone.0225380> (2019).
- Wishart, D. S. Applications of metabolomics in drug discovery and development. *Drugs R D* **9**, 307–322. <https://doi.org/10.2165/00126839-200809050-00002> (2008).
- Duan, L. et al. Application of metabolomics in toxicity evaluation of traditional Chinese medicines. *Chin. Med.* **13** <https://doi.org/10.1186/s13020-018-0216-6> (2018).
- Sillé, F. & Hartung, T. Metabolomics in preclinical drug safety assessment: current status and future trends. *Metabolites* **14**, 98. <https://doi.org/10.3390/metabo14020098> (2024).
- Züllig, T. et al. A metabolomics workflow for analyzing complex biological samples using a combined method of untargeted and target-list based approaches. *Metabolites* **10**, 342. <https://doi.org/10.3390/metabo10090342> (2020).
- Lu, Y., Pang, Z. & Xia, J. Comprehensive investigation of pathway enrichment methods for functional interpretation of LC–MS global metabolomics data. *Brief. Bioinform.* **24**, bbac553. <https://doi.org/10.1093/bib/bbad007> (2023).
- Treudler, R. & Simon, J. C. Anaphylaxis to food additives. *Allergo J. Int.* **31**, 141–144. <https://doi.org/10.1007/s40629-022-00203-y> (2022).
- Zhang, J. et al. Appropriate ammonium-nitrate ratio improves nutrient accumulation and fruit quality in pepper (*Capsicum annuum* L.). *Agronomy* **9**, 683. <https://doi.org/10.3390/agronomy9110683> (2019).
- Lugo-González, J. C., Gómez-Tagle, P., Flores-Alamo, M. & Yatsimirsky, A. K. Mechanistic study of carboxylic acid and phosphate ester cleavage by oximate metal complexes surpassing the limiting reactivity of highly basic free oximate anions. *Dalton Trans.* **49**, 2452–2467. <https://doi.org/10.1039/C9DT04733F> (2020).
- Badea, G. I. & Radu, G. L. *Carboxylic Acid - Key Role in Life Sciences*. IntechOpen, (2018).
- Kanehisa, M., Furumichi, M., Sato, Y., Matsuura, Y. & Ishiguro-Watanabe, M. KEGG: biological systems database as a model of the real world. *Nucleic Acids Res.* **53**, 672–677. <https://doi.org/10.1093/nar/gkac909> (2025).
- Olesti, E., González-Ruiz, V., Wilks, M. F. & Rudaz, S. Approaches in metabolomics for regulatory toxicology applications. *Analyst* **146**, 1820–1834. <https://doi.org/10.1039/D0AN02212H> (2021).
- Martínez-Sena, T., Quintás, G. & Saura, D. The assessment of the potential hepatotoxicity of new drugs by in vitro metabolomics. *Front. Pharmacol.* **14**, 98. <https://doi.org/10.3389/fphar.2023.1155271> (2023).
- Creydt, M. & Fischer, M. Food metabolomics: latest hardware developments for non-targeted food authenticity. *Electrophoresis* **43**, 1569–1581. <https://doi.org/10.1002/elps.202200126> (2022).
- Zhang, J. et al. Emerging trends and applications of metabolomics in food science and nutrition. *Food Funct.* **14**, 9050–9082. <https://doi.org/10.1039/D3FO01770B> (2023).
- Gupta, R. & Gaur, S. LC-MS investigated as a tool to study the metabolomic characteristics of cereal fermentation. *Appl. Food Res.* **4**, 100365. <https://doi.org/10.1016/j.afres.2023.100365> (2024).
- Rodríguez-Morató, J., Pozo, O. J. & Marcos, J. Targeting human urinary metabolome by LC-MS/MS: a review. *Bioanalysis* **10**, 489–516. <https://doi.org/10.4155/bio-2017-0285> (2018).
- Panseri, S. et al. Impact of irradiation on metabolomics profile of ground meat and its implications toward food safety. *LWT-Food Sci. Technol.* **161**, 113305. <https://doi.org/10.1016/j.lwt.2022.113305> (2022).
- Wu, W. et al. Emerging applications of metabolomics in food science and future trends. *Food Chem. X* **16**, 100500. <https://doi.org/10.1016/j.fochx.2022.100500> (2022).
- Song, G. et al. Spatial metabolomics, LC-MS and RNA-Seq reveal the effect of red and white muscle on rabbit meat flavor. *Meat Sci.* **219**, 109671. <https://doi.org/10.1016/j.meatsci.2024.109671> (2025).
- Robertson, D. G., Watkins, P. B. & Reilly, M. D. Metabolomics in toxicology: preclinical and clinical applications. *Toxicol. Sci.* **120**, 146–170. <https://doi.org/10.1093/toxsci/kfq358> (2011).
- Castro-Puyana, M. & Herrero, M. Metabolomics approaches based on mass spectrometry for food safety, quality, and traceability. *Trends Anal. Chem.* **52**, 74–87. <https://doi.org/10.1016/j.trac.2013.05.016> (2013).
- Xu, Y. J., Wang, C., Ho, W. E. & Ong, C. N. Recent developments and applications of metabolomics in Microbiological investigations. *Trends Anal. Chem.* **56**, 37–48. <https://doi.org/10.1016/j.trac.2013.12.009> (2014).

31. Farhana, R. P. Metabolomics—the new frontier in food safety and quality research. *Food Res. Int.* **72**, 80–81. <https://doi.org/10.1016/j.foodres.2015.03.028> (2015).

Acknowledgements

This research was supported by the Bio&Medical Technology Development Program of the National Research Foundation (NRF) funded by the Korean government (MSIT) [NRF-2022M3A9I3082364].”

Author contributions

H.P. composed the contents of the paper and wrote the manuscript. K.H., Y.B., and W.S. developed the muscle satellite cell and myotube foamed cell. I.C. and S.J. analyzed the results and prepared the figures and tables. D.J. supervised the overall research, contributed to the study design, provided resources, and was responsible for critical data interpretation. All authors have participated in search of the literature, analysis and evaluation of quality, results and writing. Finally, the authors reviewed the final version of the manuscript.

Competing interests

The authors declare no competing interests.

Additional information

Supplementary Information The online version contains supplementary material available at <https://doi.org/10.1038/s41598-025-00719-7>.

Correspondence and requests for materials should be addressed to D.-W.J.

Reprints and permissions information is available at www.nature.com/reprints.

Publisher’s note Springer Nature remains neutral with regard to jurisdictional claims in published maps and institutional affiliations.

Open Access This article is licensed under a Creative Commons Attribution-NonCommercial-NoDerivatives 4.0 International License, which permits any non-commercial use, sharing, distribution and reproduction in any medium or format, as long as you give appropriate credit to the original author(s) and the source, provide a link to the Creative Commons licence, and indicate if you modified the licensed material. You do not have permission under this licence to share adapted material derived from this article or parts of it. The images or other third party material in this article are included in the article’s Creative Commons licence, unless indicated otherwise in a credit line to the material. If material is not included in the article’s Creative Commons licence and your intended use is not permitted by statutory regulation or exceeds the permitted use, you will need to obtain permission directly from the copyright holder. To view a copy of this licence, visit <http://creativecommons.org/licenses/by-nc-nd/4.0/>.

© The Author(s) 2025